Australian Journal of Basic and Applied Sciences, 4(5): 893-905, 2010
ISSN 1991-8178

Free Vibration Analysis of Functionally Graded Quadrangle Plates Using Second Order Shear Deformation Theory

[1]A. Shahrjerdi, [3]M. Bayat, [2]F. Mustapha, [1]S.M. Sapuan and [2]R. Zahari

[1]Department of Mechanical and Manufacturing Engineering, Universiti Putra Malaysia, 43400 UPM, Serdang, Selangor,Malaysia
[2]Department of Aerospace Engineering, Universiti Putra Malaysia, 43400 UPM, Serdang, Selangor, Malaysia
[3]Department of Mechanical Engineering, Universiti Putra Malaysia, 50603 Kuala Lumpur, Malaysia

Abstract: A general approach for free vibration of functionally graded materials (FGMs) plates based on second-order shear deformation theory (SSDT) is presented. Material properties are assumed to be graded in the thickness direction by power law distribution in term of the volume fractions of the constituents. The equilibrium equations are derived by energy method and then solved analytically by applying Navier's method for a plate with simply supported boundary conditions. It is found that the fundamental frequencies versus side-to-side ratio for FG quadrangular plates are between full-ceramic plate and full-metal plate. It is shown that for the grading index smaller than two (p<2) the decreasing slope of the frequency is greater than that in other parts for all values of side-to-thickness ratio in square FG plate. Natural frequencies for different mode shape are compared and verified with the known results in the literature. It is seen that the results of the second-order theory are very close to the third-order reported in the literature.

Key words: Functionally graded material; Second Order Shear Deformation; Free Vibration; Quadrangle plate

INTRODUCTION

Functionally graded materials (FGMs) are those, in which the volume fraction of the two or more materials is varied, as a power-law distribution, continuously as a function of position along certain dimension (s) of the structure (Reddy, 2000 & Suress and Movtensen, 1998). Vibration of plates is a well-established branch of research in structural dynamics. They have vast range of applications in engineering and technology. There are few works on the Vibration of functionally graded structures in contrary to the extensive investigations on isotropic and composite plates and shells.

Using finite element method (FEM), Praveen and Reddy (Praveen and Reddy, 1998), studied the static and dynamic responses of functionally graded (FG) ceramic-metal plate accounting for the transverse shear deformation, rotary inertia and moderately large rotations in the Von-Karman sense, in which effect of imposed temperature field on the response of the FG plate was discussed in detail. (Ng et al., 2000) dealt with the parametric resonance of FG rectangular plates under harmonic in-plane loading. Ferreira and Batra (Ferreira and Batra, 2006) provided a global collocation method for Natural frequencies of FG plates by a meshless method with first order shear deformation theory (FSDT). (Woo *et al,* 2006) presented an analytical solution for the nonlinear free vibration behavior of FGM plates that fundamental equations were obtained using the Von-Karman theory for large transverse deflection, and the solution was based in terms of mixed Fourier series. (Zhao *et al.,* 2008) studied free vibration analysis of metal and ceramic FG plates that used the element-free kp-Ritz method. The FSDT was employed to account for the transverse shear strain and rotary inertia, and mesh-free kernel particle functions were used to approximate the two-dimensional displacement fields and the eigen-equation was obtained by applying the Ritz procedure to the energy functional of the system. (Batra and Jin, 2005) used the FSDT coupled with the FEM to study free vibrations of a FG anisotropic rectangular plate with various edge conditions and also (Batra and Aimmanee, 2005) studied a higher order shear and normal deformable plate theory by FEM. Many studies conducted on FGMs are related to the analysis of free vibration

Corresponding Author: F. Mustapha, Department of Aerospace Engineering, Universiti Putra Malaysia, 43400 UPM, Serdang, Selangor, Malaysia
Tel.: +60389466404, Fax: +60 3 86567125 E-mail: Faizal@eng.upm.edu.my

by applying FSDT (see (Bayat *et al.,* 2007, 2008 & Heidary and Eslami, 2006) and the references there in). Another shear deformation theory such as third order-shear deformation theory (TSDT) that accounts for the transverse effects has been considered. (Cheng and Batra, 2000) applied Reddy's third order plate theory to study buckling and steady state vibrations of a simply supported FG isotropic polygonal plate and Vel and Batra (Vel and Batra, 2004) dealt with the three-dimensional exact solution for free and forced vibrations of simply supported FGM rectangular plates using FDST and TSDT by employing the power series method. Nonlinear vibration and dynamic response of FGM plates in thermal environments studied [Huang and Shen, 2008] based on the higher-order shear deformation plate theory and general Von-Karman type equation. Static analysis of FG plates using TSDT and a meshless method are presented by (Ferreira *et al.,* 2005).

As mentioned above, shear deformation theories have been applied to consider transverse shear strains and rotation. Some studies apply second-order shear deformation theory (SSDT). (Khdeir and Reddy, 1999) studied the free vibration of laminated composite plates using SSDT. (Bahtuei and Eslami, 2007) also investigated the coupled thermoelastic response of a FG circular cylindrical shell by considering SSDT.

To the authors' knowledge, a few works has been done in the area of dynamic stability of FGM plate by using SSDT. In this study, the free vibration of FG plates (rectangular and square) by using SSDT is presented. The material properties of plates are graded along the thickness direction according to a volume fraction power law distribution. The classical elasticity is considered and the complete governing equations are presented. Navier's method is applied to solve equations. This work aims to investigate the effect of some basic factors such as material properties, side-to-side and side-to-thickness ratio for FG quadrangular plates on simply support boundary conditions.

Gradation Relations:

There are some models in the literature that express the variation of material properties in FGMs. The most commonly used of these models is the power law distribution of the volume fraction. According to this model, the material property gradation through the thickness of the plate is assumed to be the following form (Bayat *et al.,* 2007):

$$E = E(x_3) = (E_c - E_m)(x_3/h + 1/2)^p + E_m \tag{1a}$$

$$\rho = \rho(x_3) = (\rho_c - \rho_m)(x_3/h + 1/2)^p + \rho_m \tag{2b}$$

Here E and ρ denote the modulus of elasticity and density of FG structure, while these parameters come with subscript m or c represent the material properties for pure metal and pure ceramic plate respectively. The thickness coordinate variable is presented by x_3 while, $-\frac{h}{2} \le x_3 \le \frac{h}{2}$ where h is the total thickness of the plate as shown in Figure 1. $p \ge 0$ is the volume fraction exponent (also called grading index in this paper); $(x_3/h + 1/2)^p$ denotes the volume fraction of the ceramic.

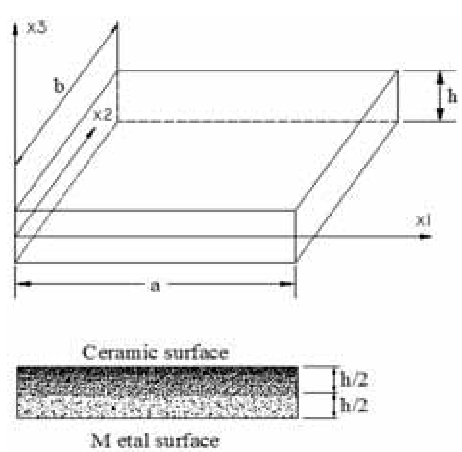

Fig. 1: Functionally graded plate.

A FG rectangular is considered as shown in Figure 1. The material in top surface and in bottom surface is Full-Ceramic and Full-Metal respectively, and between these two pure materials, power law distribution of material is applied. The most well-known FGM is compositionally graded from a ceramic to a metal to incorporate such diverse properties as heat, wear and oxidation resistance of ceramics with the toughness, strength, machinability and bending capability of metals[7].

Elastic Equations:

Consider a thin FG plate with constant thickness h, width, a, and length, b, as shown in Figure 1. Cartesian coordinate system (x_1,$x2x$,x_3) is used.

1 Displacement Field and Strains:

The SSDT is based on the following representation of the displacement field:

$$u_1 = u + x_3\phi_1 + x_3^2\phi_2 \tag{2a}$$

$$u_2 = v + x_3\psi_1 + x_3^2\psi_2 \tag{2b}$$

$$u_3 = w \tag{2c}$$

Where (u_1, u_2, u_3) denote the displacement components in the (x_1, x_2, x_3) directions respectively; (u,v,w) are the displacements of a point on the mid plane (x_1, x_2, 0). All displacement components

($u, v, w, \phi_1, \phi_2, \psi_1, \psi_2$) are functions of position (x_1, x_2) and time t.

The strain-displacement equations of the linear strain are given by (Reddy, 2007).

$$\begin{Bmatrix}\varepsilon_{11}\\ \varepsilon_{22}\\ \gamma_{12}\end{Bmatrix} = \begin{Bmatrix}\varepsilon_{11}^0\\ \varepsilon_{22}^0\\ \varepsilon_{12}^0\end{Bmatrix} + x_3\begin{Bmatrix}\kappa_{11}\\ \kappa_{22}\\ \kappa_{12}\end{Bmatrix} + x_3^2\begin{Bmatrix}\kappa_{11}^{'}\\ \kappa_{22}^{'}\\ \kappa_{12}^{'}\end{Bmatrix} \tag{3a}$$

$$\begin{Bmatrix}\gamma_{23}\\ \gamma_{13}\end{Bmatrix} = \begin{Bmatrix}\gamma_{23}^0\\ \gamma_{13}^0\end{Bmatrix} + x_3\begin{Bmatrix}\gamma_{23}^1\\ \gamma_{13}^1\end{Bmatrix} \tag{3b}$$

where

$$\begin{aligned}
&\varepsilon_{11}^0 = \frac{\partial u}{\partial x_1}, \kappa_{11} = \frac{\partial \phi_1}{\partial x_1}, \kappa_{11}^{'} = \frac{\partial \phi_2}{\partial x_1}\\
&\varepsilon_{22}^0 = \frac{\partial v}{\partial x_2}, \kappa_{22} = \frac{\partial \psi_1}{\partial x_2}, \kappa_{22}^{'} = \frac{\partial \psi_2}{\partial x_2}\\
&\varepsilon_{12}^0 = \frac{\partial u}{\partial x_2} + \frac{\partial v}{\partial x_1}, \kappa_{12} = \frac{\partial \phi_1}{\partial x_2} + \frac{\partial \psi_1}{\partial x_1}, \kappa_{12}^{'} = \frac{\partial \phi_2}{\partial x_2} + \frac{\partial \psi_2}{\partial x_1}\\
&\gamma_{23}^0 = \psi_1 + \frac{\partial w}{\partial x_2}, \gamma_{13}^0 = \phi_1 + \frac{\partial w}{\partial x_1}, \gamma_{23}^1 = 2\psi_2, \gamma_{13}^1 = 2\phi_2
\end{aligned} \tag{4}$$

2. Stress-Strain Relations:

The stress-strain relations are given by (Khedeir and Reddy, 1999).

$$\begin{Bmatrix}\sigma_{11}\\ \sigma_{22}\\ \sigma_{23}\\ \sigma_{13}\\ \sigma_{12}\end{Bmatrix} = \begin{bmatrix}q_{11} & q_{12} & 0 & 0 & 0\\ q_{12} & q_{22} & 0 & 0 & 0\\ 0 & 0 & q_{44} & 0 & 0\\ 0 & 0 & 0 & q_{55} & 0\\ 0 & 0 & 0 & 0 & q_{66}\end{bmatrix}\begin{Bmatrix}\varepsilon_{11}\\ \varepsilon_{22}\\ \varepsilon_{23}\\ \varepsilon_{13}\\ \varepsilon_{12}\end{Bmatrix} \tag{5}$$

where q_{ij} are the material constants that shown

$$q_{11} = q_{22} = \frac{E}{1-\nu^2} \qquad q_{12} = \nu q_{11} \qquad q_{44} = q_{55} = q_{66} = \frac{E}{2(1+\nu)} \tag{6}$$

$$\begin{Bmatrix} \sigma_{11} \\ \sigma_{22} \\ \sigma_{23} \\ \sigma_{13} \\ \sigma_{12} \end{Bmatrix} = \begin{bmatrix} q_{11} & q_{12} & 0 & 0 & 0 \\ q_{12} & q_{22} & 0 & 0 & 0 \\ 0 & 0 & q_{66} & 0 & 0 \\ 0 & 0 & 0 & q_{55} & 0 \\ 0 & 0 & 0 & 0 & q_{44} \end{bmatrix} \left(\begin{Bmatrix} \varepsilon_{11}^0 \\ \varepsilon_{22}^0 \\ \gamma_{23}^0 \\ \gamma_{13}^0 \\ \varepsilon_{12}^0 \end{Bmatrix} + x_3 \begin{Bmatrix} \kappa_{11} \\ \kappa_{22} \\ \gamma_{23}^1 \\ \gamma_{13}^1 \\ \kappa_{12} \end{Bmatrix} + x_3^2 \begin{Bmatrix} \kappa'_{11} \\ \kappa'_{22} \\ 0 \\ 0 \\ \kappa'_{12} \end{Bmatrix} \right) \tag{7}$$

3. *Equations of Motion:*

For a rectangular plate, if K,U and V are the kinetic, strain and potential energies of the body, respectively. The summation of the potential energy of external forces and strain energy, $U+V$, is called the total potential energy, Π, of the body. The Hamilton's principle for an elastic body can be represented,

$$\int_{t_1}^{t_2} \left(\delta K - \delta \Pi \right) dt = 0 \tag{8}$$

The inertias are defined by

$$I_i = \int_{\frac{-h}{2}}^{\frac{h}{2}} \rho_0 \left(x_3 \right)^i dx_3 \qquad \left(i = 0,1,2,\ldots,6 \right) \tag{9}$$

Hamilton's principle, equation (8), by considering SSDT, equations (2), yields the complete form of the equilibrium equations:

$$\begin{aligned}
&\frac{\partial N_{11}}{\partial x_1} + \frac{\partial N_{12}}{\partial x_2} = I_0 \ddot{u} + I_2 \ddot{\phi}_2 + I_1 \ddot{\phi}_1 \\
&\frac{\partial N_{22}}{\partial x_2} + \frac{\partial N_{12}}{\partial x_1} = I_0 \ddot{v} + I_2 \ddot{\psi}_2 + I_1 \ddot{\psi}_1 \\
&\frac{\partial Q_{13}}{\partial x_1} + \frac{\partial Q_{23}}{\partial x_2} = I_0 \ddot{w} \\
&\frac{\partial M_{11}}{\partial x_1} + \frac{\partial M_{12}}{\partial x_2} - Q_{13} = I_2 \ddot{\phi}_1 + I_1 \ddot{u} + I_3 \ddot{\phi}_2 \\
&\frac{\partial L_{11}}{\partial x_1} + \frac{\partial L_{12}}{\partial x_2} - 2R_{13} = I_2 \ddot{u} + I_4 \ddot{\phi}_2 + I_3 \ddot{\phi}_1 \\
&\frac{\partial M_{22}}{\partial x_2} + \frac{\partial M_{12}}{\partial x_1} - Q_{23} = I_2 \ddot{\psi}_1 + I_1 \ddot{v} + I_3 \ddot{\psi}_2 \\
&\frac{\partial L_{22}}{\partial x_2} + \frac{\partial L_{12}}{\partial x_1} - 2R_{23} = I_2 \ddot{v} + I_4 \ddot{\psi}_2 + I_3 \ddot{\psi}_1
\end{aligned} \tag{10}$$

where N,M,L,Q are the stress resultants. These parameters can be present by

$$\begin{Bmatrix} N_{11} \\ N_{22} \\ N_{12} \end{Bmatrix} = \int_{-\frac{h}{2}}^{\frac{h}{2}} \begin{Bmatrix} \sigma_{11} \\ \sigma_{22} \\ \sigma_{12} \end{Bmatrix} dx_3 \quad , \begin{Bmatrix} N_{11} \\ N_{22} \\ N_{12} \end{Bmatrix} = \begin{bmatrix} A_{11}\varepsilon_{11}^0 + B_{11}\kappa_{11} + D_{11}\kappa_{11}^{'} + A_{12}\varepsilon_{22}^0 + B_{12}\kappa_{22} + D_{12}\kappa_{22}^{'} \\ A_{12}\varepsilon_{11}^0 + B_{12}\kappa_{11} + D_{12}\kappa_{11}^{'} + A_{22}\varepsilon_{22}^0 + B_{22}\kappa_{22} + D_{22}\kappa_{22}^{'} \\ A_{66}\varepsilon_{12}^0 + B_{66}\kappa_{12} + D_{66}\kappa_{12}^{'} \end{bmatrix} \tag{11a}$$

$$\begin{Bmatrix} M_{11} \\ M_{22} \\ M_{12} \end{Bmatrix} = \int_{-\frac{h}{2}}^{\frac{h}{2}} \begin{Bmatrix} \sigma_{11} \\ \sigma_{22} \\ \sigma_{12} \end{Bmatrix} x_3 dx_3 \quad , \begin{Bmatrix} M_{11} \\ M_{22} \\ M_{12} \end{Bmatrix} = \begin{bmatrix} B_{11}\varepsilon_{11}^0 + D_{11}\kappa_{11} + E_{11}\kappa_{11}^{'} + B_{12}\varepsilon_{22}^0 + D_{12}\kappa_{22} + E_{12}\kappa_{22}^{'} \\ B_{12}\varepsilon_{11}^0 + D_{12}\kappa_{11} + E_{12}\kappa_{11}^{'} + B_{22}\varepsilon_{22}^0 + D_{22}\kappa_{22} + E_{22}\kappa_{22}^{'} \\ B_{66}\varepsilon_{12}^0 + D_{66}\kappa_{12} + E_{66}\kappa_{12}^{'} \end{bmatrix} \tag{11b}$$

$$\begin{Bmatrix} L_{11} \\ L_{22} \\ L_{12} \end{Bmatrix} = \int_{-\frac{h}{2}}^{\frac{h}{2}} \begin{Bmatrix} \sigma_{11} \\ \sigma_{22} \\ \sigma_{12} \end{Bmatrix} x^2{}_3 dx_3 , \quad \begin{Bmatrix} L_{11} \\ L_{22} \\ L_{12} \end{Bmatrix} = \begin{bmatrix} D_{11}\varepsilon_{11}^0 + E_{11}\kappa_{11} + F_{11}\kappa_{11}^{'} + D_{12}\varepsilon_{22}^0 + E_{12}\kappa_{22} + F_{12}\kappa_{22}^{'} \\ D_{12}\varepsilon_{11}^0 + E_{12}\kappa_{11} + F_{12}\kappa_{11}^{'} + D_{22}\varepsilon_{22}^0 + E_{22}\kappa_{22} + F_{22}\kappa_{22}^{'} \\ D_{66}\varepsilon_{12}^0 + E_{66}\kappa_{12} + F_{66}\kappa_{12}^{'} \end{bmatrix} \tag{11c}$$

$$\begin{Bmatrix} Q_{13} \\ Q_{23} \end{Bmatrix} = \int_{-\frac{h}{2}}^{\frac{h}{2}} \begin{Bmatrix} \sigma_{13} \\ \sigma_{23} \end{Bmatrix} dx_3 , \quad \begin{Bmatrix} Q_{13} \\ Q_{23} \end{Bmatrix} = \begin{bmatrix} A_{55}\gamma_{13}^0 + B_{55}\gamma_{13}^1 \\ A_{44}\gamma_{23}^0 + B_{44}\gamma_{23}^1 \end{bmatrix} \tag{11d}$$

$$\begin{Bmatrix} R_{13} \\ R_{23} \end{Bmatrix} = \int_{-\frac{h}{2}}^{\frac{h}{2}} \begin{Bmatrix} \sigma_{13} \\ \sigma_{23} \end{Bmatrix} x_3 dx_3 , \quad \begin{Bmatrix} R_{13} \\ R_{23} \end{Bmatrix} = \begin{bmatrix} B_{55}\gamma_{13}^0 + D_{55}\gamma_{13}^1 \\ B_{44}\gamma_{23}^0 + D_{44}\gamma_{23}^1 \end{bmatrix} \tag{11e}$$

where

$$A_{ij}, B_{ij}, D_{ij}, E_{ij}, F_{ij} = \int_{-\frac{h}{2}}^{\frac{h}{2}} q_{ij}\left(1, x_3, x_3^2, x_3^3, x_3^4\right) dx_3 \tag{12a}$$

Here $A_{ij}, B_{ij}, D_{ij}, E_{ij}\ and\ F_{ij}$ are plate stiffness.

$$\text{For} \begin{cases} A_{ij}, D_{ij}, F_{ij} & (i,\ j = 1, 2, 4, 5, 6) \\ E_{ij}, B_{ij} & (i,\ j = 1, 2, 6) \end{cases} \tag{12b}$$

By substituting equations (4) into equations (11) and then into equations (10) and also by applying definition (12) the Navier's equation for FG plates are obtained as follow:

$$\begin{aligned} & A_{11}\frac{\partial^2 u}{\partial x_1^2} + A_{66}\frac{\partial^2 u}{\partial x_2^2} + \left(A_{12} + A_{66}\right)\frac{\partial^2 v}{\partial x_1 \partial x_2} + B_{11}\frac{\partial^2 \phi_1}{\partial x_1^2} + B_{66}\frac{\partial^2 \phi_1}{\partial x_2^2} + D_{11}\frac{\partial^2 \phi_2}{\partial x_1^2} + \\ & D_{66}\frac{\partial^2 \phi_2}{\partial x_2^2} + \left(B_{12} + B_{66}\right)\frac{\partial^2 \psi_1}{\partial x_1 \partial x_2} + \left(D_{12} + D_{66}\right)\frac{\partial^2 \psi_2}{\partial x_1 \partial x_2} = I_0 \ddot{u} + I_2 \ddot{\phi}_2 + I_1 \ddot{\phi} \end{aligned} \tag{13a}$$

$$\begin{aligned} & A_{12}\frac{\partial^2 u}{\partial x_1 \partial x_2} + A_{66}\frac{\partial^2 u}{\partial x_1 \partial x_2} + A_{22}\frac{\partial^2 v}{\partial x_2^2} + A_{66}\frac{\partial^2 v}{\partial x_1^2} + (B_{12} + B_{66})\frac{\partial^2 \phi_1}{\partial x_1 \partial x_2} + (D_{12} + D_{66})\frac{\partial^2 \phi_2}{\partial x_1 \partial x_2} \\ & + B_{66}\frac{\partial^2 \psi_1}{\partial x_1^2} + B_{22}\frac{\partial^2 \psi_1}{\partial x_2^2} + D_{66}\frac{\partial^2 \psi_2}{\partial x_1^2} + D_{22}\frac{\partial^2 \psi_2}{\partial x_2^2} = I_0 \ddot{v} + I_2 \ddot{\psi}_2 + I_1 \ddot{\psi}_1 \end{aligned} \tag{13b}$$

$$A_{55}\frac{\partial \phi_1}{\partial x_1} + A_{55}\frac{\partial^2 w}{\partial x_1^2} + 2B_{55}\frac{\partial \phi_2}{\partial x_1} + A_{44}\frac{\partial \psi_1}{\partial x_2} + A_{44}\frac{\partial^2 w}{\partial x_2^2} + 2B_{44}\frac{\partial \psi_2}{\partial x_2} = I_0 \ddot{w} \tag{13c}$$

$$B_{11}\frac{\partial^2 u}{\partial x_1^2} + B_{66}\frac{\partial^2 u}{\partial x_2^2} + \left(B_{12}+B_{66}\right)\frac{\partial^2 v}{\partial x_1 \partial x_2} + D_{11}\frac{\partial^2 \phi_1}{\partial x_1^2} + D_{66}\frac{\partial^2 \phi_1}{\partial x_2^2} + E_{11}\frac{\partial^2 \phi_2}{\partial x_1^2} + E_{66}\frac{\partial^2 \phi_2}{\partial x_2^2}$$
$$+\left(D_{12}+D_{66}\right)\frac{\partial^2 \psi_1}{\partial x_1 \partial x_2} + \left(E_{12}+E_{66}\right)\frac{\partial^2 \psi_2}{\partial x_1 \partial x_2} - A_{55}\left(\frac{\partial w}{\partial x_1}\right) - A_{55}\phi_1 - 2B_{55}\phi_2 = I_2\ddot{\phi}_1 + I_1\ddot{u} + I_3\ddot{\phi}_2 \tag{13d}$$

$$D_{11}\frac{\partial^2 u}{\partial x_1^2} + D_{66}\frac{\partial^2 u}{\partial x_2^2} + D_{12}\frac{\partial^2 v}{\partial x_1 \partial x_2} + E_{11}\frac{\partial^2 \phi_1}{\partial x_1^2} + E_{66}\frac{\partial^2 \phi_1}{\partial x_2^2} + F_{11}\frac{\partial^2 \phi_2}{\partial x_1^2} + F_{66}\frac{\partial^2 \phi_2}{\partial x_2^2}$$
$$+\left(E_{12}+E_{66}\right)\frac{\partial^2 \psi_1}{\partial x_1 \partial x_2} + \left(F_{12}+F_{66}\right)\frac{\partial^2 \psi_2}{\partial x_1 \partial x_2} - 2\left(B_{55}\left(\frac{\partial w}{\partial x_1}\right) + 2D_{55}\phi_2 + B_{55}\phi_1\right) = I_2\ddot{u} + I_4\ddot{\phi}_2 + \tag{13e}$$

$$\left(B_{12}+B_{66}\right)\frac{\partial^2 u}{\partial x_1 \partial x_2} + B_{22}\frac{\partial^2 v}{\partial x_1^2} + B_{66}\frac{\partial^2 v}{\partial x_2^2} - A_{44}\frac{\partial w}{\partial x_2} + \left(D_{12}+D_{66}\right)\frac{\partial^2 \phi_1}{\partial x_1 \partial x_2} + \left(E_{12}+E_{66}\right)\frac{\partial^2 \phi_2}{\partial x_1 \partial x_2}$$
$$+D_{66}\frac{\partial^2 \psi_1}{\partial x_1^2} + D_{22}\frac{\partial^2 \psi_1}{\partial x_2^2} + E_{66}\frac{\partial^2 \psi_2}{\partial x_1^2} + E_{22}\frac{\partial^2 \psi_2}{\partial x_2^2} - A_{44}\psi_1 - 2B_{44}\psi_2 = I_2\ddot{\psi}_1 + I_1\ddot{v} + I_3\ddot{\psi}_2 \tag{13f}$$

$$\left(D_{12}+D_{66}\right)\frac{\partial^2 u}{\partial x_1 \partial x_2} + D_{66}\frac{\partial^2 v}{\partial x_1^2} + D_{22}\frac{\partial^2 v}{\partial x_2^2} - 2B_{44}\frac{\partial w}{\partial x_2} + \left(E_{12}+E_{66}\right)\frac{\partial^2 \phi_1}{\partial x_1 \partial x_2} + \left(F_{12}+F_{66}\right)\frac{\partial^2 \phi_2}{\partial x_1 \partial x_2}$$
$$+E_{66}\frac{\partial^2 \psi_1}{\partial x_1^2} + E_{22}\frac{\partial^2 \psi_1}{\partial x_2^2} + F_{66}\frac{\partial^2 \psi_2}{\partial x_1^2} + F_{22}\frac{\partial^2 \psi_2}{\partial x_2^2} - 2B_{44}\psi_1 - 4D_{44}\psi_2 = I_2\ddot{v} + I_4\ddot{\psi}_2 + I_3\ddot{\psi}_1 \tag{13g}$$

It can be noted by considering zero value for ϕ_2 & ψ_2 ı equations (10) and (13), FSDT equations can be obtained (Reddy, 2007).

Boundary Conditions:

For a FG plate with simply support boundary conditions at the edges as shown in Figure 2, the following relation can be written:

$$x_1 = 0, a \Rightarrow \begin{cases} v(0, x_2, t) = 0 \\ v(a, x_2, t) = 0 \\ \psi_1(0, x_2, t) = 0 \\ \psi_1(a, x_2, t) = 0 \\ \psi_2(0, x_2, t) = 0 \\ \psi_2(a, x_2, t) = 0 \end{cases}, \begin{cases} M_{11}(0, x_2, t) = 0 \\ N_{11}(0, x_2, t) = 0 \\ M_{11}(a, x_2, t) = 0 \\ N_{11}(a, x_2, t) = 0 \end{cases}, \begin{cases} w(0, x_2, t) = 0 \\ w(a, x_2, t) = 0 \end{cases} \tag{14a}$$

$$x_2 = 0, b \Rightarrow \begin{cases} u(x_1, 0, t) = 0 \\ u(x_1, b, t) = 0 \\ \phi_1(x_1, 0, t) = 0 \\ \phi_1(x_1, b, t) = 0 \\ \phi_2(x_1, 0, t) = 0 \\ \phi_2(x_1, b, t) = 0 \end{cases}, \begin{cases} M_{22}(x_1, 0, t) = 0 \\ N_{22}(x_1, 0, t) = 0 \\ M_{22}(x_1, b, t) = 0 \\ N_{22}(x_1, b, t) = 0 \end{cases}, \begin{cases} w(x_1, 0, t) = 0 \\ w(x_1, b, t) = 0 \end{cases} \tag{14b}$$

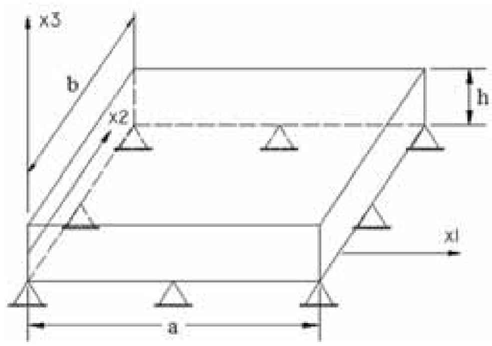

Fig. 2: Simply supported boundary condition in FG plate.

Method of Solution:

The Navier method is used for frequency analysis in the simply supported FG plate. The displacement field can be assumed:

$$u=\sum_{n=1}^{\infty}\sum_{m=1}^{\infty}u_{mn}(t)\cos\alpha x_1\sin\beta x_2 \quad ,u_{mn}(t)=Ue^{-i\omega t} \tag{15a}$$

$$v=\sum_{n=1}^{\infty}\sum_{m=1}^{\infty}v_{mn}(t)\sin\alpha x_1\cos\beta x_2 \quad ,v_{mn}(t)=Ve^{-i\omega t} \tag{15b}$$

$$w=\sum_{n=1}^{\infty}\sum_{m=1}^{\infty}w_{mn}(t)\sin\alpha x_1\sin\beta x_2 \quad ,w_{mn}(t)=We^{-i\omega t} \tag{15c}$$

$$\phi_1=\sum_{n=1}^{\infty}\sum_{m=1}^{\infty}\phi_{1mn}(t)\cos\alpha x_1\sin\beta x_2 \quad ,\phi_{1mn}(t)=\Phi_1e^{-i\omega t} \tag{15d}$$

$$\phi_2=\sum_{n=1}^{\infty}\sum_{m=1}^{\infty}\phi_{2mn}(t)\cos\alpha x_1\sin\beta x_2 \quad ,\phi_{2mn}(t)=\Phi_2e^{-i\omega t} \tag{15e}$$

$$\psi_1=\sum_{n=1}^{\infty}\sum_{m=1}^{\infty}\psi_{1mn}(t)\sin\alpha x_1\cos\beta x_2 \quad ,\psi_{1mn}(t)=\Psi_1e^{-i\omega t} \tag{15f}$$

$$\psi_2=\sum_{n=1}^{\infty}\sum_{m=1}^{\infty}\psi_{2mn}(t)\sin\alpha x_1\cos\beta x_2 \quad ,\psi_{2mn}(t)=\Psi_2e^{-i\omega t} \tag{15g}$$

where

$$\alpha=\frac{m\pi}{a} \quad ,\beta=\frac{n\pi}{b} \tag{16}$$

For natural vibration, substituting equations (15) into equations of motion (13), these equations reduce to the following forms:

$$[C]\begin{Bmatrix}U\\V\\W\\\Phi_1\\\Phi_2\\\psi_1\\\psi_2\end{Bmatrix}-\omega^2[M]\begin{Bmatrix}U\\V\\W\\\Phi_1\\\Phi_2\\\psi_1\\\psi_2\end{Bmatrix}=\begin{Bmatrix}0\\0\\0\\0\\0\\0\\0\end{Bmatrix} \tag{17}$$

where ω is natural frequency and

$$
\begin{array}{lll}
C_{11} = A_{11}\alpha^2 + A_{66}\beta^2 & C_{21} = (A_{12} + A_{66})\alpha\beta & C_{31} = 0 \\
C_{12} = (A_{12} + A_{66})\alpha\beta & C_{22} = A_{66}\alpha^2 + A_{22}\beta^2 & C_{32} = 0 \\
C_{13} = 0 & C_{23} = 0 & C_{33} = A_{55}\alpha^2 + A_{44}\beta^2 \\
C_{14} = B_{11}\alpha^2 + B_{66}\beta^2 \; , & C_{24} = (B_{12} + B_{66})\alpha\beta \; , & C_{34} = A_{55}\alpha \\
C_{15} = D_{11}\alpha^2 + D_{66}\beta^2 & C_{25} = (D_{12} + D_{66})\alpha\beta & C_{35} = 2B_{55}\alpha \\
C_{16} = (B_{12} + B_{66})\alpha\beta & C_{26} = B_{66}\alpha^2 + B_{22}\beta^2 & C_{36} = A_{44}\beta \\
C_{17} = (D_{12} + D_{66})\alpha\beta & C_{27} = D_{66}\alpha^2 + D_{22}\beta^2 & C_{37} = 2B_{44}\beta
\end{array}
$$

$$
\begin{array}{ll}
C_{41} = B_{11}\alpha^2 + B_{66}\beta^2 & C_{51} = D_{11}\alpha^2 + D_{66}\beta^2 \\
C_{42} = (B_{12} + B_{66})\alpha\beta & C_{52} = (D_{12} + D_{66})\alpha\beta \\
C_{43} = A_{55}\alpha & C_{53} = 2B_{55}\alpha \\
C_{44} = D_{11}\alpha^2 + D_{66}\beta^2 + A_{55} & C_{54} = E_{11}\alpha^2 + E_{66}\beta^2 + 2B_{55} \; , \\
C_{45} = E_{11}\alpha^2 + E_{66}\beta^2 + 2B_{55} & C_{55} = F_{11}\alpha^2 + F_{66}\beta^2 + 4D_{55} \\
C_{46} = (D_{12} + D_{66})\alpha\beta & C_{56} = (E_{12} + E_{66})\alpha\beta \\
C_{47} = (E_{12} + E_{66})\alpha\beta & C_{57} = (F_{12} + F_{66})\alpha\beta
\end{array}
$$

$$
\begin{array}{ll}
C_{61} = (B_{12} + B_{66})\alpha\beta & C_{71} = (D_{12} + D_{66})\alpha\beta \\
C_{62} = B_{66}\alpha^2 + B_{22}\beta^2 & C_{72} = D_{66}\alpha^2 + D_{22}\beta^2 \\
C_{63} = A_{44}\beta & C_{73} = 2B_{44}\beta \\
C_{64} = (D_{12} + D_{66})\alpha\beta & C_{74} = (E_{12} + E_{66})\alpha\beta \\
C_{65} = (E_{12} + E_{66})\alpha\beta & C_{75} = (F_{12} + F_{66})\alpha\beta \\
C_{66} = D_{66}\alpha^2 + D_{22}\beta^2 + A_{44} & C_{76} = E_{66}\alpha^2 + E_{22}\beta^2 + 2B_{44} \\
C_{67} = E_{66}\alpha^2 + E_{22}\beta^2 + 2B_{44} & C_{77} = F_{66}\alpha^2 + F_{22}\beta^2 + 4D_{44}
\end{array}
\tag{18}
$$

By considering relations (18), equation (17) can be written as:

$$\left| C_{ij} - M_{ij}\omega^2 \right| = 0 \tag{19}$$

By solving equation (19) and consider appropriate values for *n and m* in equation (16) the fundamental frequency of quadrangle FG plate can be obtained.

Validation and Numerical Results:

1. Validation:

The results for FG plate that obtain by applying SSDT in this study are compared with the results obtained by using TSDT in Ref (Ferreira, 2006) and exact solution of (Vel and Batra, 2004). The following non-dimensional fundamental frequencies in Table 1 and Table 2 are obtained by considering material properties the same as (Ferreira, 2006).

Results in table 1 and Table 2 show that the values that obtain by SSDT are greater than those from TSDT and exact solution. This is due to the fact that the transverse shear and rotary inertia will have more effect on a thicker plate. For the thick plates considered in this case, there is an insignificant difference between the result predicted by SSDT and TSDT; SSDT slightly over predicts frequencies. It can be seen that there are good agreement between our results and other results.

Table 1: Non-dimensional fundamental frequency $(\bar{\omega} = \omega h\sqrt{\frac{\rho_m}{E_m}})$ of a simply supported square (Al/Zro2) FG plate (P=1).

h/a=0.05			*h/a*=0.1			*h/a*=0.2		
Present study	Ref. (Ferreira, 2006)	Exact (Vel, 2004)	Present study	Ref. (Ferreira, 2006)	Exact (Vel, 2004)	Present study	Ref. (Ferreira, 2006)	Exact (Vel, 2004)
0.0158	0.0147	0.0153	0.0621	0.0592	0.0596	0.2306	0.2188	0.2192

Table 2: Non-dimensional fundamental frequency $(\bar{\omega} = \omega h\sqrt{\frac{\rho_m}{E_m}})$ of a simply supported square (Al/Zro2) FG Plate, thickness-to-side is: *h/a*=0.2

P=2			*P*=3			*P*=5		
Present study	Ref. (Ferreira, 2006)	Exact (Vel, 2004)	Present Study	Ref. (Ferreira, 2006)	Exact (Vel, 2004)	Present Study	Ref. (Ferreira, 2006)	Exact (Vel, 2004)
0.2292	0.2188	0.2197	0.2306	0.2202	0.2211	0.2324	0.2215	0.2225

2. Numerical Example:

For numerical illustration of the free vibration of quadrangle FG plate with Zirconia as upper-surface ceramic and aluminum as lower-surface metal is considered the same as (Bayat *et al.,* 2007):

Table 3: Properties of materials used in the numerical example.

Material property	E(*Gpa*)	$\rho(Kg/m^3)$	v
Zirconia, Ceramic	211.0	4500	0.33
Aluminum, Metal	68.9	2700	0.33

2.1. Results and Discussion for the First Tenth Modes in Quadrangular Fg Plates:

In the following Tables, free frequencies are presented in non-dimensional form for square and rectangular FG plates.

Table 4 shows the non-dimensional frequency in square FG plates. It can be noted that for the same values of grading index *P*, the natural frequency increases with the increase of the mode. The effect of grading index can be shown by comparing the frequency value for the fixed value of mode and changing the values of grading index *P*. It is seen that the frequency decreases with the increase of the grading index.

Table 4: Variation of the frequency parameter $(\bar{\omega} = \omega a^2 / h\sqrt{\rho_c / E_c})$ with the grading index (P) for square Al/ZrO_2FG square plates (*a/h=10,a=b*).

m×n	mode	*p*=0	*p*=0.5	*p*=1	*p*=2	*p*=5	*p*=8	*p*=10
1x1	1	5.84	5.335	5.100	4.959	4.922	4.874	4.836
1x2	2	14.014	12.81	12.242	11.878	11.745	11.623	11.534
2x1	3	14.014	12.81	12.242	11.878	11.745	11.623	11.534
2x2	4	21.58	19.766	18.89	18.301	18.041	17.841	17.702
2x3	5	33.140	30.444	29.101	28.111	27.622	27.287	27.078
3x2	6	33.140	30.444	29.101	28.111	27.622	27.287	27.078
3x3	7	43.66	40.201	38.429	37.093	36.299	35.832	35.544
3x4	8	57.084	52.674	50.359	48.580	47.313	46.702	46.315
4x3	9	57.084	52.674	50.359	48.580	47.313	46.702	46.315
4x4	10	69.29	64.109	61.321	59.022	57.382	56.532	56.059

Table 5 shows the non-dimensional frequency in rectangular FG plates. The effect of grading index can be shown by comparing the frequency for the same value of mode and considering different values of grading index *P* as shown in Table 5. It is seen that the frequency decreases with the increase of the grading index. For the same value of *P*, it can be said that the natural frequency increases with the increase of the mode. By Comparing Tables 5 and 4 it can be observed that for the same values of grading index and mode, the fundamental frequency in square FG plates are greater than those in rectangular FG plates.

2.2. Results and Discussion for the Nature Frequency in Quadrangular FG Plates:

Figures (3) and (4) illustrate the non-dimensional frequency versus grading index (*P*), for different values of side-to-thickness ratio (*a/h*) and side-to-side ratio (*b/a*), respectively.

In Figure 3, the effect of grading index (*P*) and side-to-thickness ratio (*a/h*) on fundamental frequency is shown. It can be seen that the frequency decreases with the increase of the grading index. It can be absorbed the natural frequency is maximum for full-ceramic (*p*=00) and this value increases with the increases of the value of side-to-thickness ratio. It is seen that for the values (*P*), while $0<P<2$ the slop is grater than other parts (P>2). It can be said that for side-to-thickness ratio greater than twenty (a/h>20) the frequency will be near to each other for different values of grading index. It can be noted that the difference between frequencies in a/h=5 and a/h=10 are greater than differences of frequency between a/h=10 and other curves for the same values of grading index$P$. And also it can be concluded for a/h>20 the difference between the frequencies is small for the same value of grading index.

Table 5: Variation of the frequency parameter $(\bar{\omega} = \omega a^2 / h\sqrt{\rho_c / E_c})$ with the grading index (P) for rectangular Al/ZrO_2FG square plates ($a/h=10, a=05\times b$).

$m\times n$ mode	p=0	p=0.5	p=1	p=2	p=5	p=8	p=10
1x1 1	3.6983	3.3713	3.2225	3.1354	3.1151	3.0854	3.0617
1x2 2	5.8498	5.3359	5.1002	4.9594	4.9220	4.8742	4.8367
2x1 3	12.0345	10.9940	10.5062	10.1985	10.0934	9.9908	9.9141
2x2 4	14.0144	12.8103	12.2421	11.8784	11.7458	11.6240	11.5345
2x3 5	17.2325	15.7660	15.0670	14.6092	14.4268	14.2726	14.1623
3x2 6	26.3462	24.1494	23.0749	22.3273	21.9736	21.7262	21.5587
3x3 7	29.2257	26.8100	25.6184	24.7781	24.3605	24.0789	23.8920
3x4 8	33.1402	30.4316	29.0821	28.1113	27.6006	27.2712	27.0576
4x3 9	44.1730	40.6369	38.8293	37.4607	36.6588	36.1996	35.9166

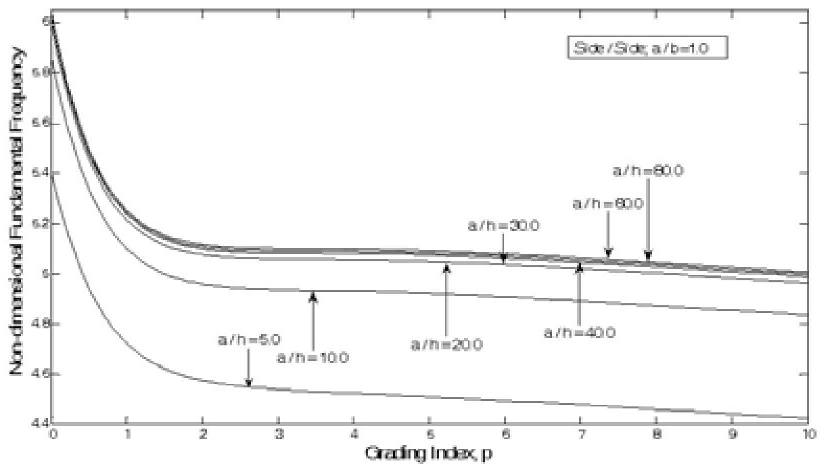

Fig. 3: Non-dimensional frequency $(\bar{\omega} = \omega a^2 / h\sqrt{\rho_c / E_c})$ versus grading index (P) for different values of side-to-thickness ration (a/h) in square FG plate.

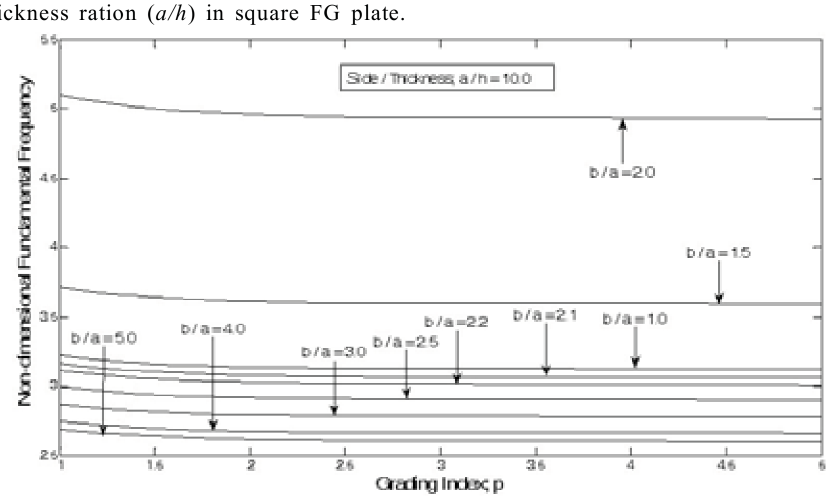

Fig. 4: Non-dimensional frequency $(\bar{\omega} = \omega a^2 / h\sqrt{\rho_c / E_c})$ versus grading index (P) for different values of side-to-side ratio (b/a) when. a/h=100

The effect of grading index (*P*) and side-to-side ratio (*b/a*) on fundamental frequency can be seen in figure 4. It can be noted that the frequency increases with the increase of the *b/a* while *b/a*<2 in contract the values of frequency decreases with the increase of the *b/a* while *b/a*>2. It can be absorbed that the frequency is almost constant for different values of grading index.

Figures (5) and (6) show variation of non-dimensional fundamental frequency with side-to-thickness ratio (*a/h*), for different values of grading index (*P*) and side-to side ratio (*b/a*), respectively.

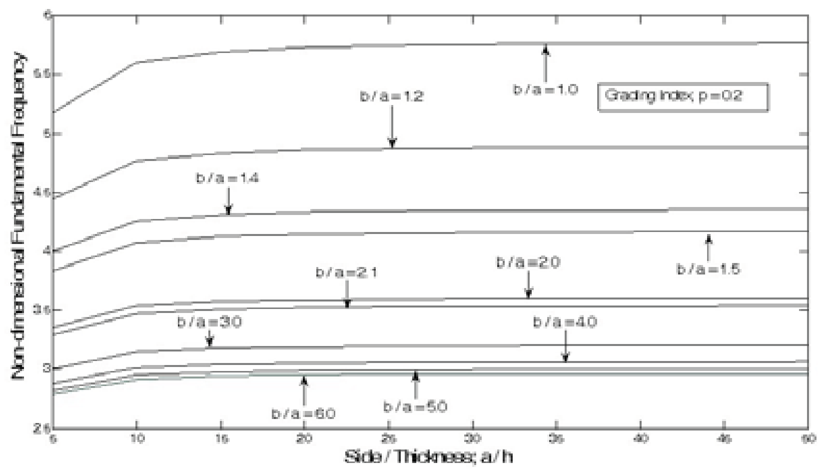

Fig. 5: Non-dimensional frequency $(\bar{\omega} = \omega a^2/h\sqrt{\rho_c/E_c})$ versus length-to-thickness (*a/h*) for different values of side-to-side ratio (*b/a*) when. *P=0.2*

It is seen from figure 5, the fundamental frequency increases with the increase of the value of side-to-thickness ratio (*a/h*). It is shown that the frequency decreases with the increase of the values of side-to-side (*b/a*). It can be noted that the slope of frequency versus side-to-thickness ratio (*a/h*) for part 5<*a/h*<10 is greater than those in another part (*a/h*>10).

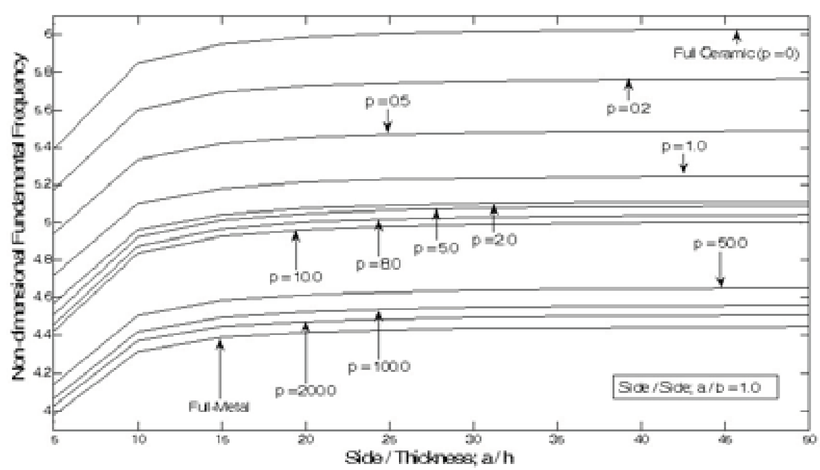

Fig. 6: Non-dimensional frequency $(\bar{\omega} = \omega a^2/h\sqrt{\rho_c/E_c})$ versus length-to-thickness (*a/h*) for different values of grading index (*P*) in square FG plates.

The variation of frequency with side-to-thickness ratio (*a/h*) for different values of grading index (*P*) is presented in Figure 6. As expected by increasing the value of grading index (*P*) the values of frequency decrease. And also the same as figure (5) whiles the 5<*a/h*<10, the slop is grater than another part. It can be noted that for the values of grading index *P*>50, the results for frequency are near two each other.

Figures 7 and 8 present the variation of non-dimensional frequency versus side-to-side ratio (*a/b*) for different values of grading index (*P*) and side-to-thickness ratio (*a/h*), respectively.

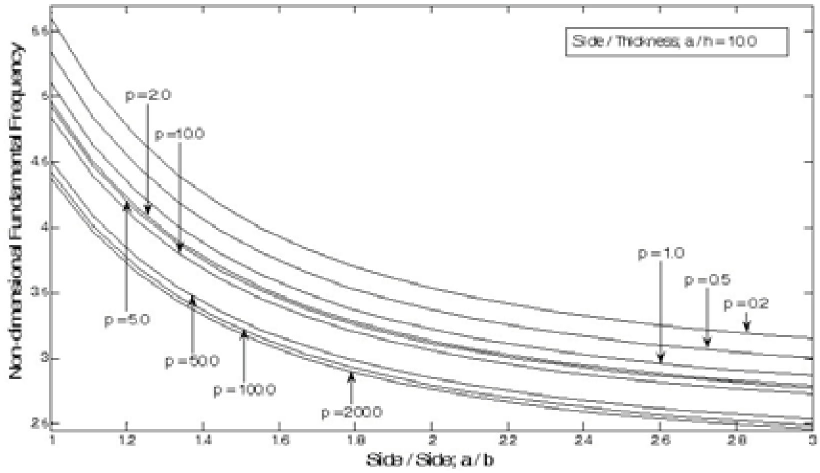

Fig. 7: Non-dimensional frequency $(\bar{\omega} = \omega a^2 / h\sqrt{\rho_c / E_c})$ versus length-to-width (*a/b*) for different values of grading index (*P*) when *a/h*=100

In figure 7, it is shown that the frequency decreases with the increase of the value of side-to-side ratio (*a/b*) for all values of grading index (*P*). It is seen the frequency for FG quadrangular plates are between full-ceramic plate and full-metal plate. As expected the frequency in full-ceramic plate is greater than those in full-metal plate.

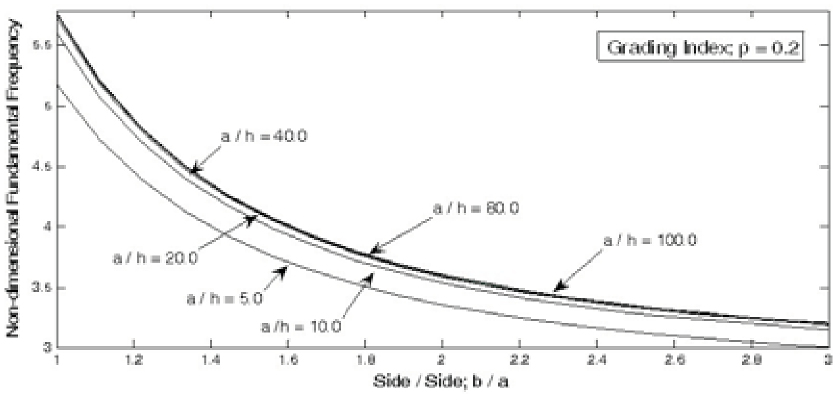

Fig. 8: Non-dimensional frequency $(\bar{\omega} = \omega a^2 / h\sqrt{\rho_c / E_c})$ versus length-to-width (*b/a*) for different values of length-to-thickness ratio (*a/h*) when *P*= 0.2.

The results for non-dimensional frequency versus side-to-side ratio (*b/a*) for different values of side-to-thickness ratio (*a/h*) in FG plate while grading index *P*=0.2 is shown in figure 8. It is seen by increasing the value of *b/a* the frequency is decreases for all values of *a/h*. It can be noted for *a/h*> the results are near to each other.

Conclusions:

Free vibration of FG quadrangular plates are investigated by applying Second order shear deformation theory (SSDT). The elastic properties of FG quadrangular plate are assumed to vary long the thickness by power law distribution. Zirconia is considered as a ceramic in upper surface while the aluminum as metal is applied for lower surface. The complete equations of motion are presented by using the Hamilton's principle. The equations are solved by using Navier's Method for simply supported FG plates.

Some general conclusions of this study can be summarized as follows:

- The slope of decreasing fundamental frequency for $0<P<2$, is greater than another part ($P>2$) for all values of side-to-thickness ratio (a/h) in square FG plate,
- For FG plates it is find that the fundamental frequency increases with the increase of the value of side-to-side ratio (b/a) when $b/a<2$ in contract, the values of frequency decrease with the increase of the b/a when $b/a>2$.
- For FG plates the slope of increasing frequency versus side-to-thickness (a/h) when $5<a/h<10$ is greater than another part ($a/h>10$) for any values of grading index and side-to-side ratio.
- The fundamental frequency versus side-to-side ratio (b/a) for FG quadrangular plates are between full-ceramic plate and full-metal plate while $a/h=10$.

From the numerical results presented in this study it can be suggested that the gradation of the constitutive components are a significant parameter in the frequency of quadrangular FG plates.

ACKNOWLEDGEMENTS

The authors would like to thank to Universiti Putra Malaysia for providing the research grant (FRGS 07-10-07-398SFR 5523398) for this research work.

REFERENCES

Bahtui, A., M.R. Eslami, 2007. Coupled thermoelasticity of functionally graded cylindrical shells. Mech Res Commun, 34(1): 1-18.

Batra, R.C., J. Jin, 2005. Natural frequencies of a functionally graded anisotropic rectangular plate .J. Sound Vibr., 282: 509-516.

Batra, R.C., S. Aimmanee, 2005. Vibrations of thick isotropic plates with higher order shear and normal deformable plate theories. Comput Struct, 83: 934-955.

Bayat, M., M. Saleem, B.B. Sahari, A.M.S. Hamouda, E. Mahdi, 2007. Thermo elastic analysis of a functionally graded rotating disk with small and large deflections. Thin-Walled Struct, 45: 677-691.

Bayat, M., B.B. Sahari, M. Saleem, A. Ali, S.V. Wong, 2008. Thermo elastic solution of a functionally graded variable thickness rotating disk with bending based on the first-order shear deformation theory. *Thin-Walled Struct*.

Cheng, Z.Q., R.C. Batra, 2000. exact correspondence between eigenvalue of membranes and functionally graded simply supported polygonal plates. J. Sound Vibr, 229(4): 879-895.

Ferreira, A.J.M., R.C. Batra, C.M.C. Roque, L.F. Qian, 2005. Martins PALS. Static analysis of functionally graded plates using third-order shear deformation theory and meshless method. *Comp Struct*, 69: 449-457.

Ferreira, A.J.M., R.C. Batra, C.M.C. Roque, L.F. Qian, R.M.N. Jorge, 2006. Natural frequencies of functionally graded plates by a meshless method. Comp Struct, 75: 593-600.

Heidary, F., M.R. Eslami, 2006. Piezo-control of forced vibrations of a thermoelastic composite plate. Comp Struct, 74(1): 99-105.

Huang, X.L., H. Shen, 2004. Nonlinear vibration and dynamic response of functionally graded plates in thermal environments. Int J. Solids Struct, 41: 2403-2427.

Khdeir, AA., J.N. Reddy, 1999. Free vibrations of laminated composite plates using second-order shear deformation theory. Comp Struct, 71: 617-626.

Ng, T.Y., K.Y. Lam, K.M. Liew., 2000. Effects of FGM materials on the parametric resonance of plate structure. *Comput. Meth Appl. Mech. Eng*, 190: 953-962.

Praveen, G.N., J.N. Reddy, 1998. Nonlinear transient thermoelastic analysis of functionally graded ceramic-metal plates.Int. J. Solids Struct, 35(33): 4457-4476.

Reddy, J.N., 2007. Theory and Analysis of Elastic Plates and Shells. CRC Press, New York.

Reddy, J.N., 2000. Analysis of functionally graded plates.*Int. J. Numer. Meth. Eng,* 47: 663-684.

Suresh, S., A. Mortensen, 1998. *Fundamentals of functionally graded materials*.IOM Communications Limited, London.

Vel, S.S., R.C. Batra, 2004. Three-dimensional exact solution for the vibration of functionally graded rectangular plates. J. Sound Vibr, 272: 703-30.

Woo, J., S.A. Meguid, L.S. Ong, 2006. Nonlinear free vibration behavior of functionally graded plates. *J. Sound Vibr*, 289: 595-611.

Zhao, X., Y.Y. Lee, K.M. Liew, 2008. Free vibration analysis of functionally graded plates using the element-free kp-Ritz method. *J. Sound Vibr*, doi:10.1016/j.jsv. 2008.06.025.